NANO LETTERS

2001
Vol. 1, No. 12
723−726

Controlling the Particle Size of Calcined SnO_2 Nanocrystals

Guangsheng Pang,*,† Siguang Chen,‡ Yuri Koltypin,‡ Arie Zaban,‡ Shouhua Feng,† and Aharon Gedanken*,‡

Department of Chemistry, Jilin University, Changchun, 130023, P. R. China, and Department of Chemistry, Bar-Ilan University, Ramat-Gan 52900, Israel

Received August 28, 2001; *Revised Manuscript Received October 1, 2001*

ABSTRACT

Smaller SnO_2 nanocrystals are prepared by a novel method. In this method, hydrous tin oxide nanoparticles are precipitated by dropping ammonium hydroxide into tin salt solution under sonication. Further calcination is conducted after the hydrous tin oxide nanoparticles are adsorbed onto the surface of $SrCO_3$ nanoparticles. Calcination at 600 °C yields SnO_2 particles with an average particle size of 3.5 nm. This compares with 5.9 nm for the sample prepared by the conventional method. The band gap of SnO_2 nanocrystals increases from 3.65 eV with a particle size 5.9 nm to 3.97 eV with a particle size 3.5 nm.

Introduction. Controlling the particle size of nanoparticles is of great technological and scientific interest. It has been demonstrated that a host of properties depend on the size of nanoparticles, including magnetic, optical, melting points, specific heats, and surface reactivity.[1,2] Furthermore, when such ultrafine particles are consolidated into a macroscale solid, these bulk materials sometimes exhibit new properties (e.g., enhanced plasticity). SnO_2 is an n-type wide band gap semiconductor with an appreciable degree of ionicity. Some unique properties of SnO_2 make this material useful for applications such as resistors, gas sensors, special coating for energy-conserving "low emissivity" windows, transparent heating elements, electrodes in glass melting furnaces, antistatic coating, etc.[3−6] Sol−gel is a common method in the preparation of SnO_2 nanoparticls.[7−10] Hydrous tin oxide is formed by hydrolysis of tin(IV) salt solutions with an average particle size between 1.5 and 3.0 nm, depending upon the preparation conditions.[7] To achieve full crystalline dehydrated product, further calcination at a high temperature is indispensable. Several strategies have been used to control the particle size of SnO_2. The use of dopant such as Nb_2O_5 can control the particle growth during the synthesis of SnO_2 processed by the polymeric precursor method.[11] Changing the surface properties by replacing the hydroxyl group with a methylsiloxyl surface group has been used to prevent the crystal growth.[12] The methylsiloxyl surface group decomposes in air at 350 °C, resulting in SiO_2 particles that serve as the "pinning" particles. The sonochemical method has also been used in the preparation of nanocrystalline SnO_2.[13]

We have developed a novel method for controlling the particle size of YSZ nanocrystalls.[14] A hydrous metal oxide colloid is precipitated from an inorganic salt solution, and a stable colloidal solution is formed after sonication in ethanol.[15] When further calcination is processed, the agglomerations of YSZ particles are inhibited after the colloidal hydrous metal oxide nanoparticles adsorbed onto the substrate of $SrCO_3$ particles. A monodispersed nanocrystalline YSZ with an average particle size of 4.7 nm is obtained. A very high surface area of 165 m^2/g and a significant band gap increase from 4.13 to 5.44 eV are observed. SnO_2 is also a very important material, and the preparation process of SnO_2 is similar to that of ZrO_2. Here, we report the preparation of nanocrystalline SnO_2 by the same method.

Experimental Section. The reactants used for the preparation of SnO_2 are $SnCl_4 \cdot 5H_2O$, $Sr(NO_3)_2$, NH_4OH, and NH_4HCO_3 (Aldrich). The synthetic process follows the experimental procedure described in ref 14. $SnCl_4 \cdot 5H_2O$ is dissolved in deionized water under stirring. Ammonium hydroxide is dropped into the solution under sonication by using a direct immersion titanium horn (Vibracell, 20 kHz, 100 W/cm^2). The precipitate is centrifuged and washed with deionized water. At this stage, the product is referred to as as-prepared hydrous SnO_2. The as-prepared hydrous SnO_2 is washed with ethanol and sonicated in ethanol for 10 min. At this stage, the product is referred to as ethanol-treated sample. $SrCO_3$ nanoparticles are prepared by dropping NH_4HCO_3 solution into 0.05 M $Sr(NO_3)_2$ solution under sonication and washed with water and ethanol. The $SrCO_3$ nanoparticles are dissolved in ethanol and formed a suspension. The $SrCO_3$ nanoparticles suspension is added into the ethanol-treated hydrous SnO_2 suspension under stirring. The

* To whom correspondence should be addressed. E-mail: gedanken@mail.biu.ac.il; panggs@mail.jl.cn.
† Jilin University.
‡ Bar-Ilan University.

10.1021/nl0156181 CCC: $20.00
Published on Web 10/11/2001

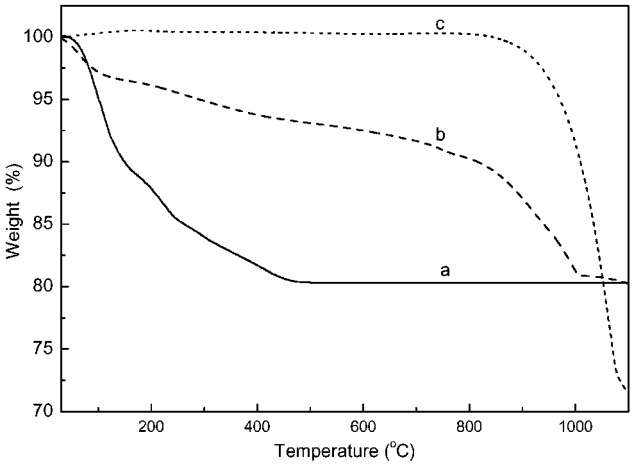

Figure 1. TGA curves of (a) the ethanol-treated hydrous SnO_2, (b) $SrCO_3$, and (c) the mixture of the ethanol-treated hydrous SnO_2 and $SrCO_3$.

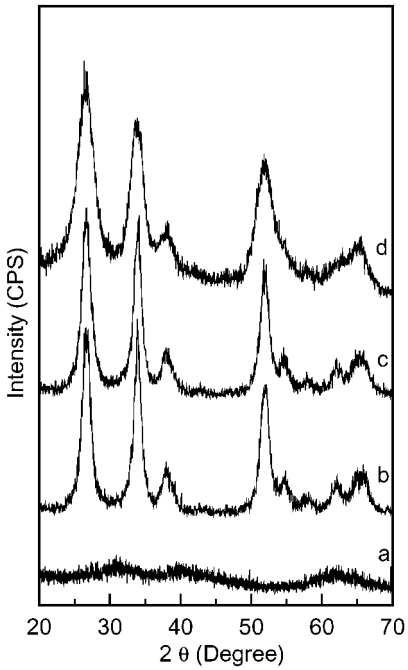

Figure 2. XRD pattern of (a) the ethanol-treated sample, (b) sample A, (c) sample B, and (d) sample C.

proportions of hydrous SnO_2 and $SrCO_3$ are 1:2.5 in weight, respectively. The mixture is further sonicated for 10 min. The mixture is evaporated by heating and stirring, dried at 120 °C, and calcined at 600 °C for 2 h. $SrCO_3$ is washed out by dissolving it in 10% HNO_3 solution under sonication. The solid product at this stage is referred to as sample C. The calcined sample of the as-prepared hydrous SnO_2 and the ethanol-treated hydrous SnO_2 are referred to as sample A and sample B, respectively.

The transmission electron micrographs (TEM) are obtained by using JEOL-JEM 100SX microscopes. Samples for TEM are prepared by placing a drop of suspension on a copper grid (400 mesh, electron microscopy sciences) coated with carbon film and then allowing it to dry in air. Powder X-ray diffraction (XRD) is performed on a Rigaku 2028 diffractometer, with nickel-filtered Cu Kα radiation. The particle size is calculated from the X-ray line broadening, using the Debye−Scherrer equation. Thermogravimetric analysis (TGA) is performed using a Mettler Toledo TGA/SDTA851 in the temperature range 30−1100 °C in a nitrogen atmosphere at a heating rate of 10 °C/min. UV−vis diffuse reflectance spectroscopy (DRS) is measured by a Cary 500 UV−visible spectophotometer at room temperature in the wavelength region between 200 and 800 nm.

Results and Discussion. Parts a−c of Figure 1 show the TGA curves of the ethanol-treated hydrous SnO_2, the mixture of the ethanol-treated hydrous SnO_2 and $SrCO_3$, and $SrCO_3$, respectively. For the ethanol-treated sample, there is a weight loss of 19.7 wt % when the sample is heated from room temperature to 480 °C. Weight loss of 9.3 wt % when the sample is heated from room temperature to 130 °C is due to desorption of physical adsorbed water. The weight loss of 5.5 wt %, which occurs when the sample is heated from 130 to 250 °C, is mainly due to the loss of hydroxyl groups. The weight loss of 5.3 wt % in the temperature range 250−480 °C, is due to the removal of chemically adsorbed water and the oxidative decomposition of chemisorbed ethoxy group. The three stages of weight losses are consistent with the reported results of EXAFS study of the structural evolution during isothermal sintering of SnO_2 xerogels.[16] The small microcrystallites with the incipient cassiterite structure are formed at 110 °C, the dehydration reaction between 110 and 250 °C leads to an amorphization evidenced by a decrease of the long and short-range crystallographic order, and a continuous coagulation of the crystallites leads to grain growth at higher temperature. The pure $SrCO_3$ nanoparticles decompose at 1000 °C. The TGA curve of the mixture of ethanol-treated hydrous SnO_2 and $SrCO_3$ reveals both the dehydration of hydrous SnO_2 from room temperature to 500 °C and the decomposition of $SrCO_3$ from 700 to 1000 °C. The decomposition temperature of $SrCO_3$ decreased due to mixing with SnO_2. However, there is no obvious weight loss between 500 and 600 °C. This means that the hydrous SnO_2 can be dehydrated and crystallized at 600 °C, whereas the $SrCO_3$ nanoparticles do not decompose.

Figure 2a shows the XRD pattern of the ethanol-treated sample, which indicates its amorphous structure. The ethanol-treated hydrous SnO_2 shows the properties of an α-oxide. There are two types of hydrous tin(IV) oxide that are formed by hydrolysis of tin(IV) salt solutions depending on the conditions: the freshly prepared material is called α-oxide, which is not a crystalline product, while the aging process produces β-oxide, which has an X-ray diffraction pattern characteristic of tin(IV) oxide.[17] Sonication of $SnCl_4$ aqueous solution at 80 °C for 2 h also results in a crystalline hydrous product.[7] Parts b and c of Figure 2 show the XRD patterns of samples A and B, respectively. The particle sizes estimated from the broadening of the XRD are the same, 5.9 nm, for both samples A and B. Washing by ethanol has no effect on the particle size. This is different from the result of the calcination of hydrous YSZ.[14] For the calcination of hydrous YSZ, washing with ethanol plays an important role in the condensation process of surface hydroxyl groups. The

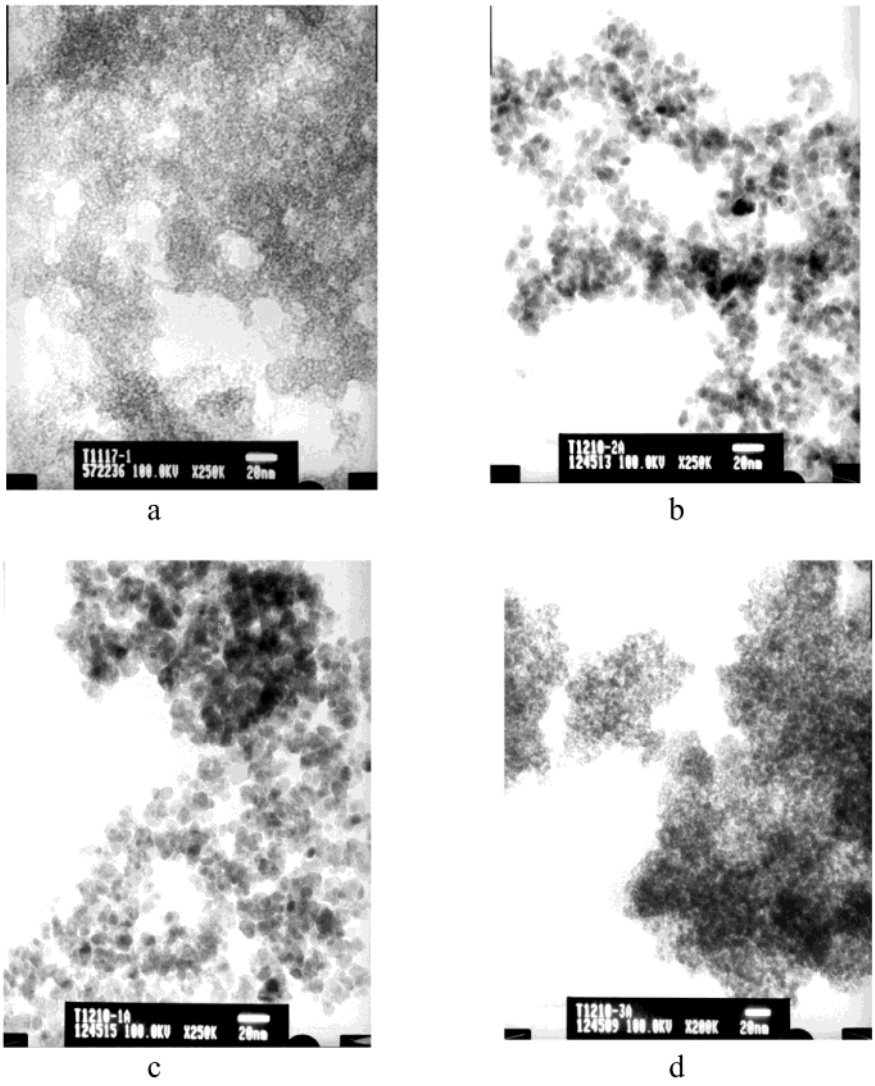

Figure 3. TEM micrographs of (a) an ethanol-treated hydrous SnO_2, (b) sample A, (c) sample B, and (d) sample C.

agglomeration and particle size of the ethanol-treated sample are significantly lower and smaller than those of the as-prepared sample. Figure 3d shows the XRD pattern of sample C. The average particle size of sample C as estimated from the broadening of the XRD is 3.5 nm.

Figure 3a shows the TEM micrographs of an ethanol-treated sample. The particles are monodispersed with a particle size of ca. 2.0 nm. Parts b and c of Figure 3 show the TEM micrographs of samples A and B, both of which consist of monodispersed particles with a particle size of ca. 6.0 nm. By comparison, the particle size of sample C is ca. 3.5 nm (Figure 3d). This size is in excellent agreement with the size calculated for sample C from the XRD data.

For semiconducting nanoparticles, the quantum confinement effect is expected, and the absorption edge will be shifted to a higher energy when the particle size decreases. The band gaps of the SnO_2 samples are studied by UV−vis diffuse reflectance spectroscopy (DRS). The Kubelka−Munk function, $F(R) = (1 - R)^2/2R$, is used to determine the band gap by analyzing the DRS results. Figure 4 shows the plots of $F(R)$ vs wavelength of samples A−C. The band gaps are

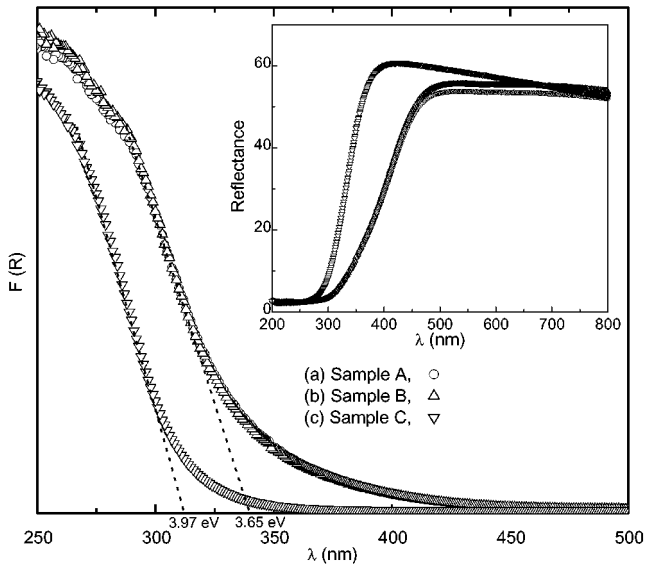

Figure 4. Plots of $F(R)$ vs wavelength of (a) sample A, (b) sample B, and (c) sample C. The inset show the DRS result.

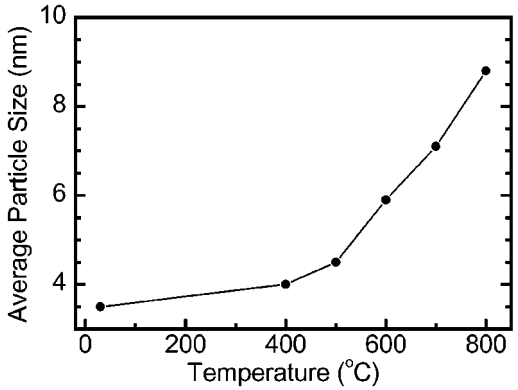

Figure 5. Variation of the average particle size of sample C after heating at different temperatures for 2 h.

defined by extrapolation of the rising part of the plots to the *X*-axis (dotted line in Figure 4). The inset of Figure 4 shows the DRS results. The band gaps of samples A−C are 3.65 eV (340 nm), 3.65 eV (340 nm), and 3.97 eV (312 nm), respectively. The band gap of the samples A and B (3.65 eV) are similar to the literature value of the bulk SnO_2.[12,18] The band gap increases from 3.65 to 3.97 eV when the particle size decreases from 5.9 to 3.5 nm.

The thermal stability of sample C is studied by heating at different temperatures for 2 h. The average particle sizes estimated from the broadening of the XRD are 4.0, 4.5, 5.9, 7.1, and 8.8 nm for the samples calcined at 400, 500, 600, 700, and 800 °C, respectively. Figure 5 shows the variation of the average particle size of sample C after heating at different temperatures. When the $SrCO_3$ is dissolved out, sample C with particle size 3.5 nm cannot be stabilized at high temperature. The particle size of sample C increases slowly to 4.5 nm at 500 °C and then increases quickly to 8.8 nm at 800 °C. It is worth noting that the particle size of sample C calcined at 600 °C is the same as that of samples A and B. This indicates that the $SrCO_3$ nanoparticles play an important role in stabilizing the smaller size nanoparticles. The effect of $SrCO_3$ inhibiting particle growth is not well understood yet. But, it is clear that there should be some interaction (such as electrostatic forces) between the SnO_2 particles and the surface of $SrCO_3$. This is also supported by the result that the decomposition temperature of $SrCO_3$ decreased when it was mixed with hydrous SnO_2 nanoparticles (Figure 1).

Conclusion. In summary, we prepared smaller nanoparticles of SnO_2 by a novel method. $SrCO_3$ plays important roles in this method. The hydrous SnO_2 nanoparticles are adsorbed onto the surface of $SrCO_3$ nanoparticles. Dispersing the hydrous SnO_2 particles on a higher surface area lowers the agglomeration and oxolation during the dehydration process. For the same precursor, temperature is an important factor to influence the particle size during the calcination process. Our results suggest that, at the same calcination temperature, changing the local environment of the precursor particles can inhibit the growth of nanocrystals. A smaller crystal size of SnO_2 usually confers good properties. An improved sensor device performance is expected for our samples.

Acknowledgment. A.G. thanks the BMBF, Germany, for financial support through the Energy Program. S.C. and G.P. thank the Kort 100 Scholarship Foundation for supporting their postdoctoral fellowship.

References

(1) Interrante, L. V.; Hampden-Smith, M. J. *Chemistry of Advanced Materials*; Wiley-VCH: New York, 1998; p 271.
(2) Alivisatos, A. P. *J. Phys. Chem.* **1996**, *100*, 13226.
(3) Ogawa, H.; Abe, A.; Nishikawa, M.; Hayakawa, S. *J. Electrochem. Soc.* **1981**, *128*, 2020.
(4) Arfsten, N. J.; Kaufmann, R.; Dislich, H. *Proc. International Conference on Ultrastructure Processing of Ceramics Glass and Composites, Gainesville, FL, 1983;* Wiley: New York, 1984; p 189.
(5) Jarzebski, Z. M.; Marton, J. P. *J. Electrochem. Soc.* **1976**, *123*, 299c.
(6) Jarzebski, Z. M.; Marton, J. P. *J. Electrochem. Soc.* **1976**, *123*, 333c.
(7) Hiratsuka, R. S.; Pulcinelli, S. H.; Santilli, C. V. *J. Non-Cryst. Solids* **1990**, *121*, 76.
(8) Pulcinelli, S. H.; Santilli, C. V.; Jolivet, J. P.; Tronc, E. *J. Non-Cryst. Solids* **1994**, *170*, 21.
(9) Briois, V.; Santilli, C. V.; Pulcinelli, S. H.; Brito, G. E. S. *J. Non-Cryst. Solids* **1995**, *191*, 17.
(10) Vincent, C. A.; Weston, D. G. C. *J. Electrochem. Soc.* **1972**, *119*, 518.
(11) Leite, E. R.; Weber, I. T.; Longo, E.; Varela, J. A. *Adv. Mater.* **2000**, *12*, 965.
(12) Wu, N.-L.; Wang, S.-Y.; Rusakova, I. A. *Sience* **1999**, *285*, 1375.
(13) Zhu, J.; Lu, Z.; Aruna, S. T.; Aurbach, D.; Gedanken, A. *Chem. Mater.* **2000**, *12*, 2557.
(14) Pang, G.; Chen, S.; Zhu, Y.; Palchik, O.; Koltypin, Yu.; Zaban, A.; Gedanken, A. *J. Phys. Chem. B* **2001**, *105*, 4647.
(15) Pang, G.; Sominska, E.; Colfen, H.; Mastai, Y.; Avivi, S.; Koltypin, Yu.; Zaban, A.; Gedanken, A. *Langmuir* **2001**, *17*, 3223.
(16) Brito, G. E. S.; Briois, V.; Pulcinelli, S. H.; Santilli, C. V. *J. Sol−Gel Sci. Technol.* **1997**, *8*, 269.
(17) Rochow, E. G.; Abel, E. W. *The Chemistry of Germanium, Tin and Lead*; Pergamon Texts in Inorganic Chemistry, Vol. 14; Pergamon Press: Oxford, U.K., 1973; p 64.
(18) Vogel, R.; Hoyer, P.; Weller, H. *J. Phys. Chem.* **1994**, *98*, 3183.

NL0156181